arXiv:1511.00039v1 [physics.chem-ph] 30 Oct 2015

Theory of diffusion-influenced reactions in complex geometries

Marta Galanti[1,2,3,4], Duccio Fanelli[1,3], Francesco Piazza[4]
[1] *Università degli Studi di Firenze, Dipartimento di Fisica e Astronomia and CSDC, via G. Sansone 1, IT-50019 Sesto Fiorentino, Firenze, Italia,*
[2] *Dipartimento di Sistemi e Informatica, Università di Firenze, Via S. Marta 3, IT-50139 Florence, Italy,*[3] *INFN, Sezione di Firenze, Italia,*[4] *Université d'Orléans, Centre de Biophysique Moléculaire, CNRS-UPR4301, Rue C. Sadron, 45071, Orléans, France.*

Chemical reactions involving diffusion of reactants and subsequent chemical fixation steps are generally termed "diffusion-influenced" (DI). Virtually all biochemical processes in living media can be counted among them, together with those occurring in an ever-growing number of emerging nano-technologies. The role of the environment's geometry (obstacles, compartmentalization) and distributed reactivity (competitive reactants, traps) is key in modulating the rate constants of DI reactions, and is therefore a prime design parameter. Yet, it is a formidable challenge to build a comprehensive theory able to describe the environment's "reactive geometry". Here we show that such a theory can be built by unfolding this many-body problem through addition theorems for special functions. Our method is powerful and general and allows one to study a given DI reaction occurring in arbitrary "reactive landscapes", made of multiple spherical boundaries of given size and reactivity. Importantly, ready-to-use analytical formulas can be derived easily in most cases.

PACS numbers: 82.40.Qt, 82.39.Rt, 87.10.Ed, 02.30.Jr

Diffusion-influenced reactions (DIR) are ubiquitous in many contexts in physics, chemistry and biology [1, 2] and keep on sparking intense theoretical and computational activity in many fields [3–11]. Modern examples of emerging nanotechnologies that rely on controlled alterations of diffusion and reaction pathways in DIRs include different sorts of chemical and biochemical catalysis involving complex nano-reactors [12, 13], nanopore-based sequencing engines [14] and morphology control and surface functionalization of inorganic-based delivery vehicles for controlled intracellular drug release [15, 16].

However, while the mathematical foundations for the description of such problems have been laid nearly a century ago [17], many present-day problems of the utmost importance at both the fundamental and applied level are still challenging. Notably, arduous difficulties arise in the quantification of the important role played by the environment's *geometry* (obstacles, compartmentalization) [18] and *distributed reactivity* (patterns of competitive reaction targets or traps) in coupling transport and reaction pathways in many natural and artificial (bio)chemical reactions [1, 19, 20].

A formidable challenge in modeling environment-related effects on chemical reactions is represented by the intrinsic many-body nature of the problem. This is brought about essentially by two basic features, common to virtually all realistic situations, namely (*i*) finite density of reactants and other inert species (in biology also referred to as *macromolecular crowding* [21, 22]) and (*ii*) confining geometry of natural or artificial reaction domains in $3D$ space. In general, the presence of multiple reactive and non-reactive particles/boundaries cannot be neglected in the study of (bio)chemical reactions occurring in real *milieux*, where the geometrical *compactness* of the environment may have profound effects, such as first-passage times that are non-trivially influenced by the starting point [23]. Relevant complex media include the cell cytoplasm [8, 24–26], porous or other artificial confining media [23, 27–32], which be considered as offering important tunable features for technological applications [12, 14, 16].

In this paper, we take a major step forward by solving the general problem of computing the steady-state reaction rate constant for a diffusion-influenced chemical reaction between a mobile ligand and an *explicit* arbitrary, static $3D$ configuration of spherical reactive boundaries of arbitrary sizes and intrinsic reactivities.

To set the stage for the forthcoming discussion, let us first consider the simple problem of two molecules A and B of size R and a, respectively, diffusing in solution. Upon encountering, the two species can form a complex, which catalyzes the transformation of species B into some product P with rate constant k,

$$A + B \xrightarrow{k} A + P \tag{1}$$

Under the hypotheses that (*i*) A molecules diffuse much more slowly than B molecules, (*ii*) both species are highly diluted and (*iii*) the bulk concentration of A molecules ρ_A is much smaller than the bulk concentration of B molecules ρ_B [2, 33], the rate constant k can be computed by solving the following stationary two-body boundary problem [1]

$$\bigtriangledown^2 u = 0 \quad \text{with} \quad u|_{\partial\Omega_0} = 0,\ \lim_{r\to\infty} u = 1 \tag{2}$$

where $\partial\Omega_0$ is a spherical sink of radius $\sigma = R + a$ (the encounter distance) and $u(r) = \rho(r)/\rho_B$ is the stationary normalized concentration of B molecules around the sink. The rate constant is simply the total flux into the sink,

i.e.

$$k = D \int\limits_{\partial\Omega_0} \left.\frac{\partial u}{\partial r}\right|_{r=\sigma} dS \tag{3}$$

where $D = D_A + D_B$ is the relative diffusion constant. The solution to the boundary problem (2) is $u(r) = 1-\sigma/r$, which yields the so-called Smoluchowski rate constant for an isolated spherical sink, namely $k_S = 4\pi D\sigma$. These simple ideas, originally developed to describe coagulation in colloidal systems [17, 34], together with the related subsequent major advances by Debye [35] and Collins & Kimball [36] represent the basic building block of many modern theoretical approaches in chemicaland soft-matter [37, 38] kinetics.

In many realistic situations in chemical and biochemical kinetics, a single ligand (B) molecule has to diffuse among *many* competing reactive particles A. In addition, it might be forced to find its target within a specific confining geometry, which in principle can be modeled through a collection of reflecting boundaries. Such settings define a genuinely many-body problem, as the overall flux of ligands is shaped by the mutual screening among all the different reactive boundaries (the *reactive environment*), known as *diffusive interaction* [39–41]. In the following we show how this kind of problems can be formulated and solved in a rather general form.

Let us imagine a reaction of the kind (1) to be catalyzed at $N+1$ spherical boundaries $\partial\Omega_\alpha$ of radius (encounter distance) $\sigma_\alpha = R_\alpha + a$, $\alpha = 0, 1, \ldots, N$ arranged in space at positions $\boldsymbol{X}_\alpha$. With reference to the Smoluchowski problem, this means that we are explicitly relaxing the assumption of vanishing density of the reactive centers A. In the most general setting, each sphere can be endowed with an intrinsic reaction rate constant k^*_α, that specifies the conversion rate from encounter complex to product at its surface. Then, the stationary density of B molecules is the solution of the following boundary value problem

$$\bigtriangledown^2 u = 0 \tag{4a}$$

$$\left(\sigma_\alpha \frac{\partial u}{\partial r_\alpha} - h_\alpha u\right)\Big|_{\partial\Omega_\alpha} = 0 \qquad \alpha = 0, 1, \ldots, N \tag{4b}$$

$$\lim_{r\to\infty} u = 1 \tag{4c}$$

where $h_\alpha = k^*_\alpha/k_{S_\alpha}$ with $k_{S_\alpha} = 4\pi D\sigma_\alpha$. The boundary conditions (BC) (4b) are called *radiative* or Robin boundary conditions. The limits $h_\alpha \to \infty$ and $h_\alpha = 0$ correspond to perfectly absorbing (sink) and reflecting (obstacle) boundaries, respectively, while values $0 < h_\alpha < \infty$ correspond to finite surface reactivity [36].

The boundary problem (4a), (4b), (4c) provides a rigorous mathematical description of a wide assortment of physical situations, ranging from one or many sinks screened by neighboring competing reactive boundaries to hindered diffusion to a sink located among a collection of static reflecting obstacles placed at given positions in space. In order to solve the problem, it is expedient to consider as many sets of spherical coordinate systems as there are boundaries, $\boldsymbol{r}_\alpha \equiv (r_\alpha, \theta_\alpha, \phi_\alpha)$. The solution can then be written formally as an expansion in series of irregular solid harmonics, namely

$$u = 1 + \sum_{\alpha=0}^{N} u^-_\alpha(\boldsymbol{r}_\alpha), \qquad u^-_\alpha = \sum_{\ell=0}^{\infty}\sum_{m=-\ell}^{\ell} \frac{B^\alpha_{m\ell}}{r^{\ell+1}_\alpha} Y_{m\ell}(\boldsymbol{r}_\alpha) \tag{5}$$

where $Y_{m\ell}(r_\alpha, \theta_\alpha\phi_\alpha)$ are spherical harmonics expressed in the local frame centered at the α-th sphere [42].

The coefficients $B^\alpha_{m\ell}$ should be determined by imposing the BCs (4b). In order to do so, we use known addition theorems for spherical harmonics [43] to express the solution (5) in all the $N+1$ different reference frames centered at each sphere. The result is the following infinite-dimensional system of linear equations

$$B^\alpha_{gq} - \frac{(q-h_\alpha)}{(h_\alpha+q+1)}\left[\delta_{g0}\delta_{q0} + \sum_{\ell=0}^{\infty}\sum_{m=-\ell}^{\ell}\sum_{\substack{\beta=0\\ \beta\neq\alpha}}^{N} B^\beta_{m\ell} W^{\alpha\beta gq}_{m\ell}\right] = 0 \tag{6}$$

for $\alpha = 0, 1, \ldots, N$, $q = 1, 2, \ldots, \infty$ and $g = -q, ..., q$ (see supplementary material for a detailed derivation and the explicit expression of the matrix elements $W^{\alpha\beta gq}_{m\ell}$). To solve the problem one simply needs to truncate the sum on ℓ in eq. (6), by including a finite number of multipoles so as to attain the desired accuracy on the overall rate constant. In analogy to eq. (3), and taking into account the definition (5), the rate constant corresponding to a given subset of reactive boundaries $\mathcal{S}$ can be computed as

$$k = D\sum_{\alpha\in\mathcal{S}} \int\limits_{\partial\Omega_\alpha} \left.\frac{\partial u}{\partial r}\right|_{r=\sigma_\alpha} dS = -\sum_{\alpha\in\mathcal{S}} k_{S_\alpha} B^\alpha_{00} \tag{7}$$

The theoretical framework that culminates in formula (7) provides an extremely powerful tool to investigate how specific geometries of obstacles and/or competitive reactive boundaries modulate the rate constant of a given diffusion-influenced reaction.

A clear and instructive illustration of our general approach can be outlined by focussing on the simplest model of diffusion-influenced reaction, namely diffusion of a ligand to a perfect sink. Even if our method could be employed to examine far more complex *reactive geometries*, realized by assembling a large number of spherical boundaries of arbitrary sizes and reactivities, for the sake of clarity we shall specialize here to the case of a sink of radius σ surrounded by N identical spheres of radius $\sigma_1 = \lambda\sigma$ arranged randomly at a fixed distance d. This problem has been tackled recently for $\lambda = 1$ and $N \leq 4$ through a numerical finite-element (FE) method in Ref. [41]. This study provided clear-cut hints of the subtle effects brought about by the environment's geometry, but also highlighted the impossibility of brute-force numerical approaches to assess the impact of more crowded and sophisticated reactive environments.

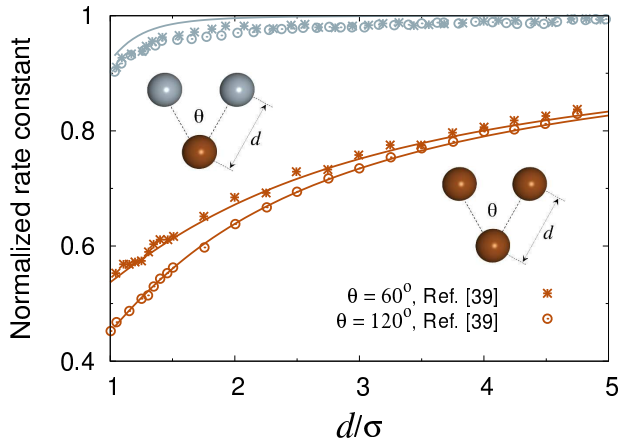

FIG. 1. **The approximate finite-element calculations compared with the exact results.** Total flux into a sink of diameter σ normalized to $k_S = 4\pi D\sigma$ (flux into an isolated sink) in the presence of two spherical screening boundaries of the same diameter placed at a fixed distance d from the sink and forming an angle θ. Light blue and dark orange denote reflecting and absorbing particles, respectively. Symbols are numerical results of finite-element calculations from Ref. [41]. Solid lines are the exact results, obtained by solving eqs. (6) with a relative accuracy of 10^{-4}.

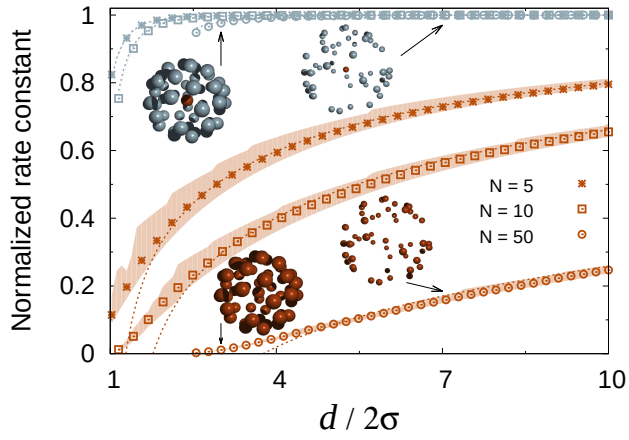

FIG. 2. **Competitive screening greatly reduces the rate constant compared to inert obstacles, and is strongly modulated by the configuration.** Total flux into a sink of radius σ surrounded by N spherical boundaries of the same size arranged randomly at distance d (normalized to $k_S = 4\pi D\sigma$). Symbols denote the exact results (solution of eqs. (6)), averaged over 100 independent configurations for each value of d. The shaded bands highlight the regions comprised between the minimum and maximum rates. For reflecting screening boundaries, these regions are as small as the truncation error. The light blue and orange lines are plots of eq. (8) and eq. (10), respectively, with $\lambda = 1$. The arrows flag values of d corresponding to the two configurations shown ($N = 50$) with the screening spheres made all absorbing (bottom) and all reflecting (top).

In Fig. 1 we compare the FE numerical results with the exact solution for $N = 2$. It appears clear that the screening effect is harder to capture via a FE scheme in the case of reflecting obstacles than in the presence of competitive sinks. However, our exact approach allows one to dig much further into this problem and investigate analytically the screening effect of configurations comprising a large number of spheres. For example, one can expand the system (6) in powers of $\varepsilon \equiv \sigma/d$ to derive simple analytical estimates of the rate constant to the sink (see supplementary material for the detailed calculations). In the case of reflecting obstacles, one gets

$$\frac{k}{k_S} = 1 - \left(\frac{\lambda^3 N}{2}\right)\varepsilon^4 - \left(\frac{2\lambda^5 N}{3}\right)\varepsilon^6 + \dots \qquad (8)$$

which is independent of the screeninig configuration and linear in N, as suggested in Ref. [41]. However, we find that this only holds up to sixth order in ε – it can be seen from the expansion that the configuration enters explicitly successive powers of ε (see supplementary material). On the other hand, a similar procedure in the case of N screening *sinks* yields

$$\frac{k}{k_s} = 1 - \lambda N\varepsilon + \left[\lambda N + \lambda^2 \sum_{\substack{\alpha,\beta=1 \\ \beta\neq\alpha}}^{N} \frac{1}{\Gamma_{\alpha\beta}}\right]\varepsilon^2 - \left[\lambda^2 N^2 + \lambda^2 \sum_{\substack{\alpha,\beta=1 \\ \beta\neq\alpha}}^{N} \frac{1}{\Gamma_{\alpha\beta}} + \lambda^3 \sum_{\substack{\alpha,\beta,\delta=1 \\ \beta,\delta\neq\alpha}}^{N} \frac{1}{\Gamma_{\alpha\beta}\Gamma_{\alpha\delta}}\right]\varepsilon^3 + \dots \qquad (9)$$

where $\Gamma_{\alpha\beta} = 2\sin(\omega_{\alpha\beta}/2)$, $\omega_{\alpha\beta}$ being the angle formed by the sinks α and β with respect to the origin. Eq. (9) makes it very clear that the configuration of competitive reactive boundaries does influence the screening effect on the central sink. A clear signature of this is also that the corrections in Eq. (9) alternate in sign. This observation sheds considerable light onto the many-body character of the rate constant, whose perturbative series is alternatively reduced by the diffusive interactions between the screening boundaries and the sink (shielding ligand flux from it) and increased by the diffusive interactions among the screening particles (shielding flux from each other). On the contrary, the screening action of inert obstacles is largely dominated by the excluded-volume effect, and thus can only yield negative corrections at all orders.

Due to its perturbative nature, eq. (9) can be used to quantify the shielding action of specific $3D$ arrangements of sinks only for $N\varepsilon \propto N/d \ll 1$. However, it still provides a powerful analytical tool to *compare* different geometries, as the perturbative rate is always proportional to the true rate (see supplementary material). For example, eq. (9) could be used to *design* the special configurations that minimize or maximize the screening effect on the central sink for given values of N and d.

The *average* shielding action exerted by N equidistant sinks can be easily obtained analytically in the

monopole approximation, *i.e.* by keeping only the $\ell = 0$ and $q = 0$ terms in eqs. (6). The ensuing reduced system can be averaged over different configurations in the hypothesis of vanishing many-body spatial correlations, *i.e.* by integrating over the probability density $\mathcal{P}_N = \prod_{\alpha\neq\beta}(\sin\omega_{\alpha\beta})/4\pi$, with $2\arcsin(\sigma_1/d) \leq \omega_{\alpha\beta} \leq \pi$ (excluded-volume constraint between screening sinks). The result is (see supplementary material for the details)

$$\left\langle \frac{k}{k_S} \right\rangle = \frac{1-\lambda\varepsilon[N-(N-1)(1-\lambda\varepsilon)]}{1-\lambda\varepsilon[N\varepsilon-(N-1)(1-\lambda\varepsilon)]} \qquad (10)$$

Fig. 2 shows that for $\lambda = 1$ eq. (10) provides an extremely good estimate of the configurational averages of the exact results at separations greater than a few diameters, highlighting the dramatic screening action of competitive reactive boundaries with respect to inert obstacles. Furthermore, a simple analysis of the rate *fluctuations* over the configuration ensembles at fixed d allows one to gauge how sensitive competitive screening is to the specific $3D$ arrangement of the sinks. Remarkably, this analysis reveals stretches between the minimum and maximum rates for a given value of d as high as 50 % of the average (see shaded bands in Fig. 2). More precisely, we remark that the variability associated with different geometries is greater (*i*) at short distances and (*ii*) for few screening particles.

Eqs. (8), (9) and (10) and the ensuing arguments are rather exemplary illustrations of the powerful analytical insight afforded by our general approach. The case of small screening sinks, $\lambda < 1$, provides a further demonstration of non-trivial effects that are captured by our analytics. It turns out that the function (10) displays a minimum for certain choices of the parameters N, λ. More precisely, a minimum exists at fixed N for $\lambda \leq \lambda^*(N) \equiv (\sqrt{4N+1}-1)/(2N) < 1$, or, alternatively, at fixed λ for $N \leq N^*(\lambda) \equiv (1-\lambda)/\lambda^2$. Fig. 3 provides a clear illustration of this subtle effect.

The flux into a large sink features a minimum for screening configurations of tiny absorbing particles close to its surface. This is the result of the competition between two effects. When the small particles lie very close to the surface of the large sink $\mathcal{S}_\sigma$, the latter behaves as an *effective isolated* sink of size $\sigma_{\rm eff} < \sigma$, absorbing a flux $\Phi_{\rm eff} = 4\pi D\sigma_{\rm eff} \lesssim k_S$. Upon increasing the distance d, the total flux to the screening sinks will increase (their *active* surfaces get larger and they also get farther apart from each other). Now it is clear that the effect of this on the flux to $\mathcal{S}_\sigma$ will depend on the size of the screening particles. If σ_1 is small enough, $\sigma_{\rm eff}$ is not much smaller than σ, so that $\Phi_{d=\sigma+\sigma_1} \equiv \Phi_{\rm eff}$ is not much smaller than $\Phi_\infty = k_S$. Under these conditions, the flux into the large sink starts *decreasing*, as the screening ensemble effectively *steal* more and more flux from it. However, upon increasing d past a critical distance, the small particles can no longer catch enough ligand flux, so that the flux to $\mathcal{S}_\sigma$ starts increasing, as it should, towards k_S.

Summarizing, in this paper we have introduced a general theoretical framework to quantify how the geometry

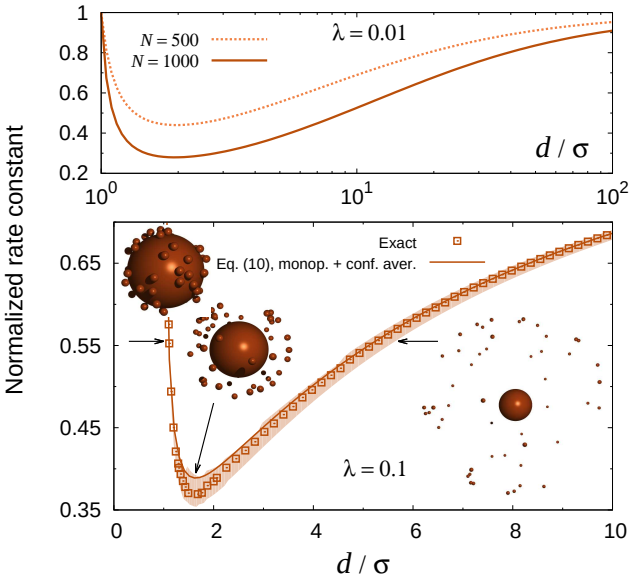

FIG. 3. **Making the screening boundaries smaller makes the flux into the sink non-monotonic**. Total flux into a sink of radius σ surrounded by $N = 50$ smaller sinks of radius $\sigma_1 = \sigma/10$ arranged randomly at a distance d (normalized to $k_S = 4\pi D\sigma$). The left-most and right-most cartoons depict two configurations that screen exactly the same amount of flux, despite being at considerably different distances ($d/\sigma = 1.1$ and $d/\sigma = 8$). The configuration shown in the middle corresponds to the predicted minimum at $d/\sigma = 1+\sqrt{1-\lambda[1+(N-1)\lambda]} \approx 1.64$. The solid line is a plot of formula (10). Each symbol is the average over 250 independent configurations, while the filled band comprises the region between the minimum and maximum rates. The top panel illustrates the case of screening by a large number of tiny particles, highlighting the sizeable non-monotonic effect. The curves are plots of eq. (10).

and distributed reactivity patterns of the environment modulate the rate constant of diffusion-influenced chemical reactions. Our method can be used to examine arbitrary *reactive landscapes*, made by assembling spherical boundaries of selected size at given locations in space and endowed with arbitrary surface reactivity. We note that our method is utterly general, as it can be easily extended to accommodate for reactive environments realized with more complex, non-spherical boundaries. The only requirement is that one of the 13 coordinate systems in which Laplace's equation is separable be used [43], and that addition theorems exist for the corresponding elementary solutions [44]. Moreover, our method can be extended to Laplace space [45], so as to work out exactly the effect of the environment on *time-dependent* problems. This technique could be employed to shed further light on the intriguing sensitivity of time-dependent effects on initial conditions, which seems to constitute a rather generic feature of complex media [23].

Finally, we stress that our method can be easily employed to derive approximate closed analytic formulas, that can be used to investigate naturally occurring re-

active geometries and to assist in the design of effective artificial nano-reactors for different technological applications.

The authors wish to thank Sergey Traytak, P. De Los Rios and G. Foffi for insightful comments. F. P. and D. F. acknowledge joint funding from the French CNRS (PICS).

[1] S. A. Rice, ed., *Diffusion-limited reactions*, Comprehensive Chemical Kinetics, Vol. 25 (Elsevier, Amsterdam, 1985).

[2] A. Szabo, The Journal of Physical Chemistry **93**, 6929 (1989).

[3] G. Foffi, A. Pastore, F. Piazza, and P. A. Temussi, Physical Biology **10**, 040301 (2013).

[4] J. Schöneberg and F. Noé, PLoS ONE **8**, e74261 EP (2013).

[5] K. Seki, M. Wojcik, and M. Tachiya, Physical review. E **85**, 011131 (2012).

[6] N. Dorsaz, C. De Michele, F. Piazza, P. De Los Rios, and G. Foffi, Physical Review Letters **105**, 120601 (2010).

[7] J. D. Schmit, E. Kamber, and J. Kondev, Physical Review Letters **102**, 218302 (2009).

[8] D. Ridgway, G. Broderick, A. Lopez-Campistrous, M. Ru'aini, P. Winter, M. Hamilton, P. Boulanger, A. Kovalenko, and M. J. Ellison, Biophysical Journal **94**, 3748 (2008).

[9] D. ben Avraham and S. Havlin, *Diffusion and Reactions in Fractals and Disordered Systems* (Cambridge University Press, 2000).

[10] S. D. Traytak, Chemical Physics **192**, 1 (1995).

[11] P. P. Mitra, P. N. Sen, L. M. Schwartz, and P. Le Doussal, Phys. Rev. Lett. **68**, 3555 (1992).

[12] Y. Lu and M. Ballauff, Progress in Polymer Science **36**, 767 (2011).

[13] N. Welsch, A. Wittemann, and M. Ballauff, Journal of Physical Chemistry B **113**, 16039 (2009).

[14] K. T. Brady and J. E. Reiner, The Journal of Chemical Physics **143**, 074904 (2015).

[15] Y. Gao, Y. Chen, X. Ji, X. He, Q. Yin, Z. Zhang, J. Shi, and Y. Li, *ACS Nano*, ACS Nano **5**, 9788 (2011).

[16] J. L. Vivero-Escoto, I. I. Slowing, B. G. Trewyn, and V. S.-Y. Lin, Small **6**, 1952 (2010).

[17] M. von Smoluchowski, Physik Z **17**, 557 (1916).

[18] O. Bénichou, C. Chevalier, J. Klafter, B. Meyer, and R. Voituriez, Nature Chemistry **2**, 472 (2010).

[19] M. F. Shlesinger, G. M. Zaslavsky, and J. Klafter, Nature **363**, 31 (1993).

[20] R. Kopelman, Science **241**, 1620 (1988).

[21] R. J. Ellis, Current Opinion in Structural Biology **11**, 114 (2001).

[22] H. X. Zhou, G. Rivas, and A. P. Minton, Annual review of biophysics **37**, 375 (2008).

[23] O. Bénichou, C. Chevalier, J. Klafter, B. Meyer, and R. Voituriez, Nature Chemistry **2**, 472 (2010).

[24] J. S. Kim and A. Yethiraj, Biophysical journal **96**, 1333 (2009).

[25] J. A. Dix and A. Verkman, Annual Review of Biophysics **37**, 247 (2008).

[26] K. Luby-Phelps, International review of cytology **192**, 189 (2000).

[27] J. Kurzidim, D. Coslovich, and G. Kahl, Journal of Physics: Condensed Matter **23**, 234122 (2011).

[28] B. Nguyen and D. Grebenkov, Journal of Statistical Physics **141**, 532 (2010).

[29] J. Kurzidim, D. Coslovich, and G. Kahl, Physical Review Letters **103**, 138303 (2009).

[30] I. L. Novak, P. Kraikivski, and B. M. Slepchenko, Biophysical Journal **97**, 758 (2009).

[31] P. S. Burada, P. Hänggi, F. Marchesoni, G. Schmid, and P. Talkner, ChemPhysChem **10**, 45 (2009).

[32] I. C. Kim and S. Torquato, The Journal of Chemical Physics **96**, 1498 (1992).

[33] F. Piazza, G. Foffi, and C. De Michele, Journal of Physics: Condensed Matter **25**, 245101 (2013).

[34] M. von Smoluchowski, Z Phys. Chem. **92**, 129 (1917).

[35] P. Debye, Transactions of The Electrochemical Society **82**, 265 (1942).

[36] F. C. Collins and G. E. Kimball, Journal of Colloid Science **4**, 425 (1949).

[37] M. Müller and N. Lebovka, "Advances in polymer science," in *Polyelectrolyte Complexes in the Dispersed and Solid State I*, Vol. 255 (Springer Berlin Heidelberg, 2014) pp. 57–96.

[38] G. Oshanin, M. Moreau, and S. Burlatsky, Advances in Colloid and Interface Science **49**, 1 (1994).

[39] S. D. Traytak, Chemical Physics Letters **197**, 247 (1992).

[40] S. D. Traytak, Chemical Physics **193**, 351 (1995).

[41] C. Eun, P. M. Kekenes-Huskey, and J. A. McCammon, Journal of Chemical Physics **139**, 044117 (2013).

[42] Here we use the definition $Y_{m\ell}(\theta,\phi) = P_\ell^m(\cos\theta)e^{im\phi}$ where $P_\ell^m(\cos\theta)$ are associated Legendre polynomials [43].

[43] P. M. Morse and H. Feshbach, *Methods of theoretical physics*, Vol. 2 (McGraw-Hill Science/Engineering/Math, 1953) pp. 409–415.

[44] E. W. Hobson, *The theory of Spherical and Ellipsoidal Harmonics* (Cambridge University Press, 1931).

[45] E. Gordeliy, S. L. Crouch, and S. G. Mogilevskaya, International Journal for Numerical Methods in Engineering **77**, 751 (2009).